*Journal of Structural Geology*, Vol 13, No 7, pp 823 to 836, 1991
Printed in Great Britain

0191-8141/91 $03 00+0 00


# Kinematics of crystal growth in syntectonic fibrous veins

J. L. URAI*

Instituut voor Aardwetenschappen, P O. Box 80021, 3508TA Utrecht, The Netherlands

P. F. WILLIAMS

Department of Geology, University of New Brunswick, Box 4400, Fredericton, N.B., Canada E3B 5A3

and

H. L. M. VAN ROERMUND†

Instituut voor Aardwetenschappen, P.O. Box 80021, 3508TA Utrecht, The Netherlands

(*Received* 21 *August* 1989; *accepted in revised form* 31 *December* 1990)

**Abstract**—Detailed observations of a set of fibrous antitaxial calcite veins in a slate reveal that some of the calcite fibres do not connect material markers on both sides of the vein and can therefore not have tracked the full opening trajectory during vein growth. This calls for a better understanding of the mechanisms of fibre formation and reliable criteria to test the tracking hypothesis. Based on surface roughness characteristics of the vein wall we develop a simple model for shape-growth of crystals in a crack–seal environment which can account for both tracking and non-tracking behaviours, and propose a set of 'tracking criteria' for antitaxial veins. Finally we discuss ways by which the model can be tested against natural examples.

## INTRODUCTION

SYNTECTONIC veins containing mineral grains with a pronounced fibrous morphology are common in rocks at metamorphic grades of greenschist facies and lower. They often occur together with veins which contain more equant infill morphologies, and are generally composed of calcite or quartz.

The fibrous morphologies are quite different from what is expected for growth of these minerals in a fluid filled cavity, where more equant growth habits are generally developed (Beach 1977).

Although it is not yet entirely clear how, repeated crack–seal events appear to play an essential role in the formation of fibrous morphologies, somehow interfering with the normal growth competition process which produces ingot textures and euhedral crystals (Grigor'ev 1965, Ramsay 1980, Cox & Etheridge 1983, van der Pluijm 1984, Cox *et al.* 1986, Mawer 1987). Note that in this paper we do not consider minerals which develop fibrous habits when growing in a free fluid.

Durney & Ramsay (1973) recognized two main types of crack–seal veins. In *antitaxial* veins crystal growth takes place with the vein filling as a substrate, *towards the wall rock*, and on only one side of the crack. In *syntaxial* veins crystals grow on the wall rock or fractured vein material, *towards the vein centre*, on both sides of the crack. Which of the two mechanisms will operate seems to depend mainly on material contrast between wall rock and vein material.

A striking feature of many vein fibres is their markedly curved shape, without the crystal lattice having the corresponding curvature. This led Durney & Ramsay (1973) to propose that the curvature was developed during crystal growth, with the fibre axis extending parallel to the opening vector of the corresponding cracking event. This gave fibrous veins great promise as a tool for deciphering progressive deformation histories in rocks, and at present fibres are a well established tool for structural geologists (Ramsay & Huber 1983, p. 235, Beutner & Diegel 1985, Ellis 1986, Passchier & Urai 1988).

Less attention has been paid to the tracking hypothesis itself, that is to ask questions like: do fibres track the incremental opening direction in all cases, by what mechanism, how does their shape reflect opening histories, and what microstructural criteria are available to test the tracking hypothesis? This is in spite of the Durney & Ramsay (1973) and Cox & Etheridge (1983) papers where examples of non-tracking fibres were convincingly described. This was further substantiated by recent papers (Cox 1987, Williams & Urai 1986, 1989) documenting more examples of veins where fibres did not track the opening direction. As the veins described by these authors have common morphologies, it is possible that the observations have a more general validity, casting doubt on results of earlier work where the tracking hypothesis was not tested.

The aim of this paper is first to give a detailed

*Present address: Koninklijke/Shell Exploratie en Productie Laboratorium, P.O. Box 60, 2280 AB Rijswijk, The Netherlands.
†Present address: Ecole Normale Superieure de Lyon, 46 Allée d'Italie, 69364 Lyon Cédex 07, France

description of a set of veins in which some fibres show microstructures consistent with the tracking hypothesis but others have not tracked the full opening trajectory, and second to propose a simple model for crystal growth in a crack–seal environment which has the potential to explain both types of behaviour.

## DATA

### *Sample description—macroscopic*

In this work we studied in detail a set of veins taken from a slate quarry on the north side of highway #4 in New York state, 3 km southwest of the New York–Vermont border. The regional geological setting is in an internally folded thrust slice, bounded by melanges of the Taconic thrust system (see Bosworth & Kidd 1985, and fig. 12 of Bosworth & Vollmer 1981 for an illustration of the large-scale structure). From the map of Bosworth & Kidd (1985) it can be seen that the quarry is located on the normal limb of a tight to isoclinal syncline–anticline pair. Passchier & Urai (1988) discussed an early set of veins from this outcrop. In this paper we concentrate on second generation veins which grew during the later stages of deformation.

The samples investigated consist of a host rock of fine-grained black slate, containing a series of quartz, calcite or mica rich layers, often less than 1 mm thick. These provide excellent markers for correlating material positions on either side of the veins. The rock is cut by up to 5 mm thick calcite veins, most of which are distinctly fibrous in hand specimen. The plane containing the curved fibres in most samples is approximately perpendicular to the intersection of bedding, cleavage and vein.

Thin sections were cut perpendicular to cleavage and contain the plane of curved fibres as accurately as could be determined in hand specimen (within a few degrees). They were doubly polished to thicknesses less than 10 $\mu$m and examined in transmitted light, cathodeluminescence (CL) and electron microscopy (backscattered SEM and TEM). Observations pertinent to this study are given below.

### *Microstructures*

Most veins are fibrous in thin section, but in a number of samples fibrous and blocky veins occur together.

*Fibrous veins.* These commonly display a well-defined median line (Durney & Ramsay 1973) defined by a thin band of fine-grained calcite, second-phase particles, and a discontinuity in the CL intensity pattern (Figs. 1–3). Calcite grains have dimensions of up to 0.1 × 0.1 × 2 mm and locally extend from vein wall to vein wall (Figs. 1e & f and 3a). More frequently they are strongly elongate but die out before reaching the other vein wall, locally because the fibre long axis is not exactly parallel to the thin section plane, or due to a discontinuity in the microstructure (Figs. 1a–c and 3b) coincident with CL zonation. Fibre thickness is quite continuous along the length of fibres which extend from wall to wall, but tends to increase from the median line towards the vein wall across the discontinuities mentioned above. Calcite grain boundaries are generally smooth and gently curved.

There are various heterogeneously distributed signs of crystal plastic deformation in some veins. Grains may show quite strong twinning and undulose extinction, the development of subgrains and rare incipient formation of new grains by grain boundary migration which tends to destroy existing CL zonations. These veins belong to the first, more strongly deformed vein generation (Passchier & Urai 1988) with a more complicated structure. They are not discussed further in this paper. Some veins have a composite structure, consisting of a deformed core with an optically undeformed outer part (e.g. Figs. 1g and 4a). The majority of veins studied in this work contain optically almost undeformed fibres with minor twinning.

Fibre curvature varies from sample to sample but is roughly consistent within each hand specimen. It is unrelated to optical deformation features. Fibres may be curved up to 90° without significant optically visible deformation features.

In CL mode the veins show a well defined banding due to discontinuities in CL intensity and colour. The banding is subparallel to the vein wall and symmetrically arranged with respect to the median line (see Fig. 1). Individual bands have shapes intermediate between those of the median line and the wall rock. In a number of examples smaller scale irregularities in wall rock shape are matched by similar irregularities in the CL banding (Fig. 1d). Discontinuities in CL intensity frequently correspond to sharp changes in fibre boundary orientations, or to the discontinuous changes in fibre thickness described above.

Using the terminations of fine-scale lithological banding at the vein wall as markers, two different types of veins can be distinguished: (i) veins in which fibres (or elongate grains) connect markers across a vein (Figs. 1e & f, 2a and 3c & d); and (ii) veins in which fibres do

Fig. 1. Transmitted light (a, c, e, g) and CL (b, d, f, h) micrographs to show vein morphologies. (a) & (b) A fibrous vein showing growth zonation symmetric about the median line. Optically undeformed fibres change thickness across CL discontinuities. Note that fibres do not accurately connect markers (M) across the vein. This vein is also shown in Fig. 2(a). The horizontal edge of each photograph is 6.8 mm. (c) & (d) CL banding (B) mimicking small-scale irregularities in the wall rock, with fibres connecting corresponding markers. Note the trail of wall rock fragments incorporated in the vein (W). This vein is also shown in Fig. 2(a). The horizontal edge of each photograph is 1 mm. (e) & (f) Optically undeformed fibres connecting markers across a small vein. Note the median line marked by CL contrast, and the thin quartz–chlorite vein at the vein tip, containing isolated calcite grains. The horizontal edge of each photograph is 1.6 mm. (g) & (h) A blocky vein with curved grain boundaries and CL banding similar to that in fibrous veins. Note the strongly twinned core overgrown by optically undeformed rim. The horizontal edge of each photograph is 0.7 mm.

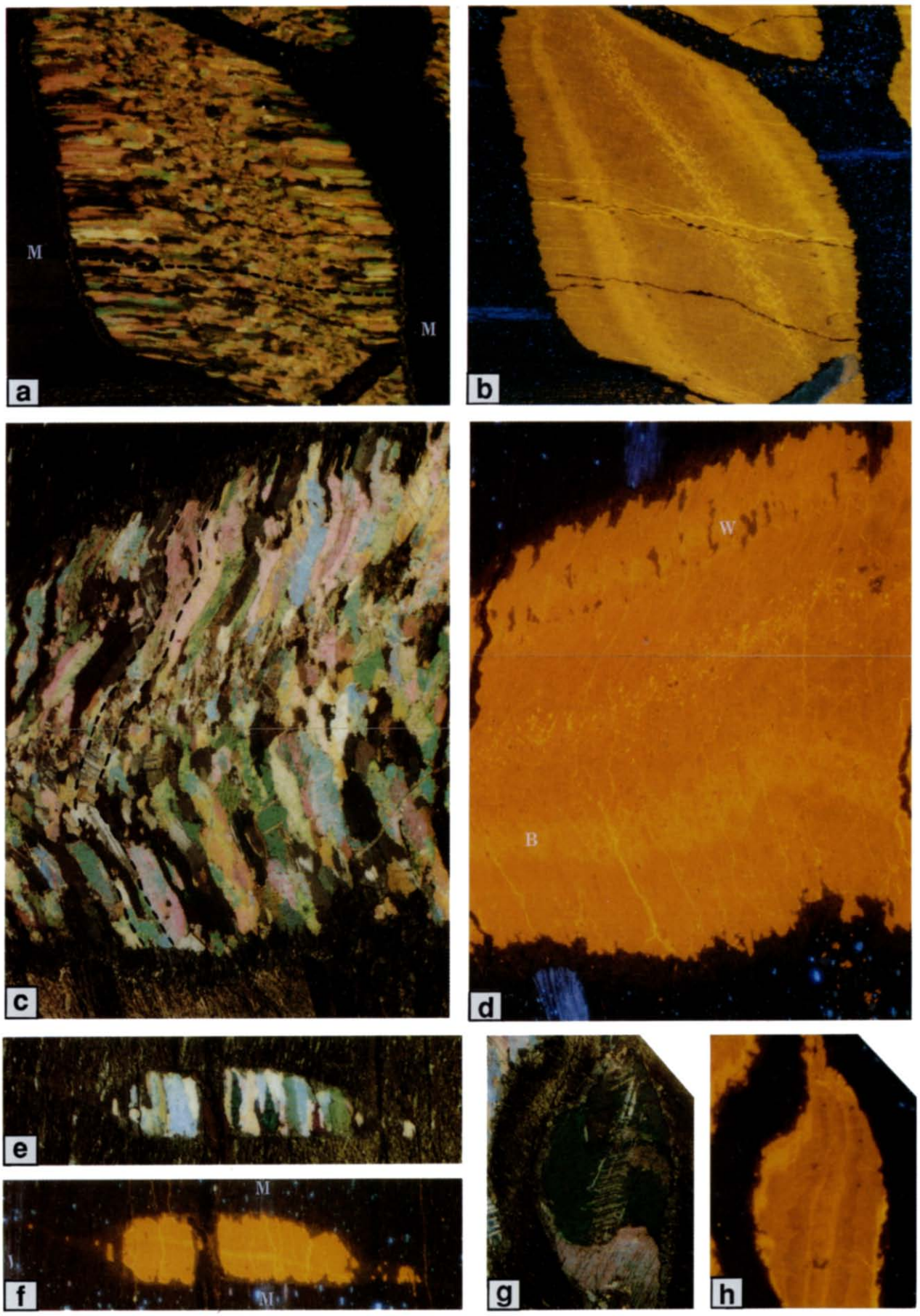


Fig. 1

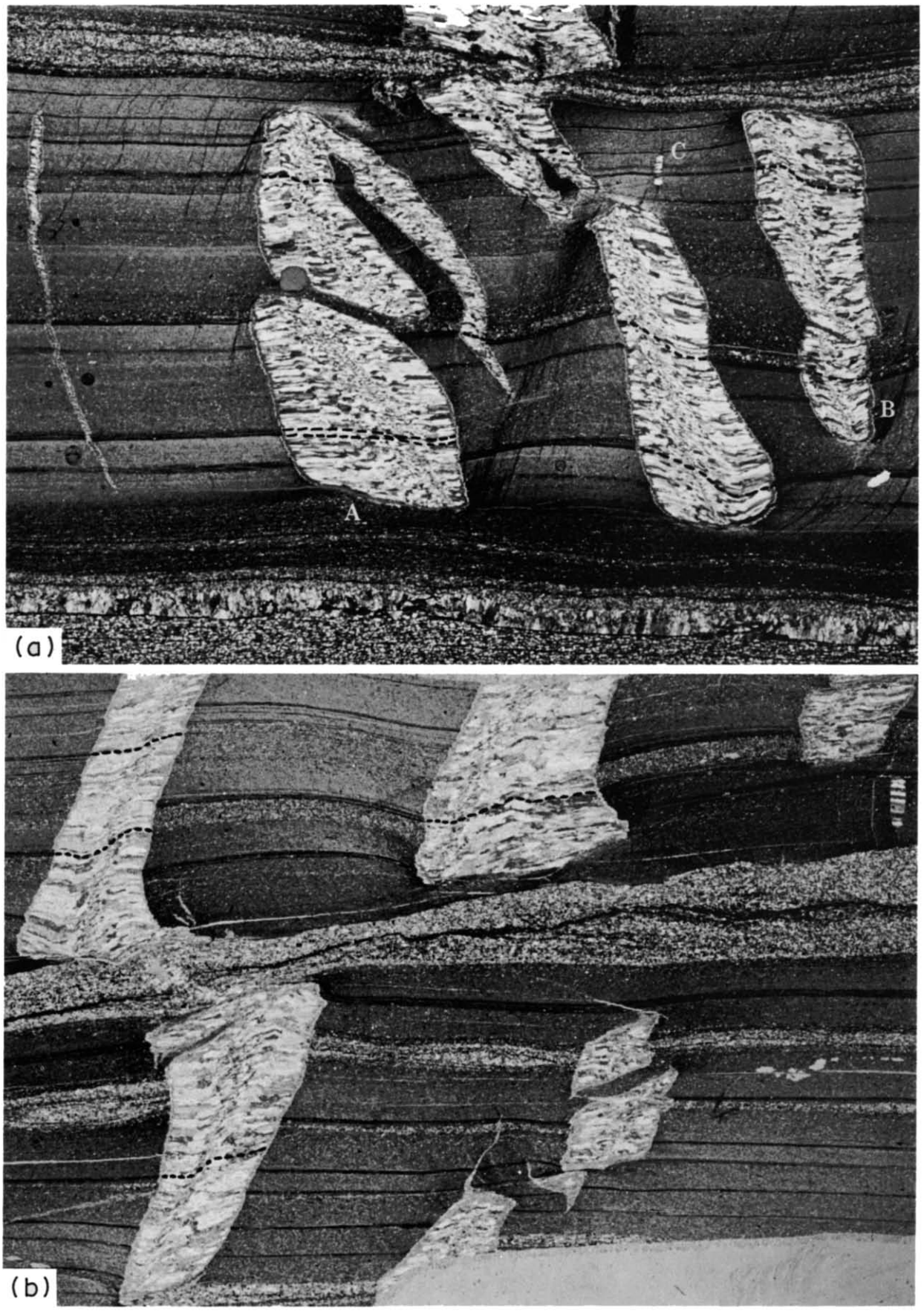


Fig. 2 (a) & (b) Micrographs showing veins in which fibres accurately connect markers, together with veins in which fibres do not connect markers Vein A is shown in detail in Fig. 1(a), vein B in Fig. 1(c) and vein C in Fig. 1(e). The long edge of each photograph is 30 mm

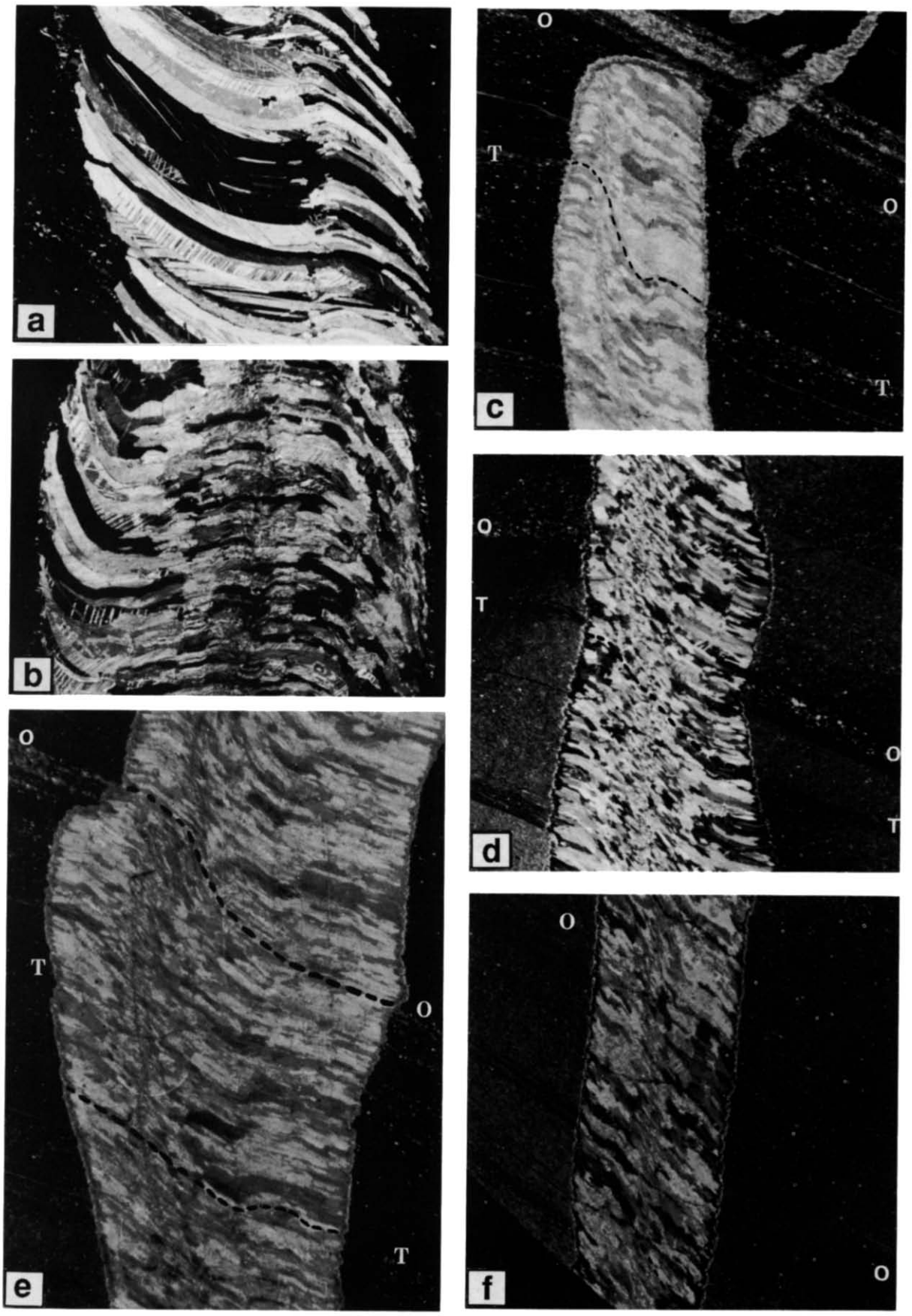


Fig. 3. (a) Fibrous vein showing curved, optically undeformed fibres extending from vein wall to vein wall, and a well defined median line. The horizontal edge of the photograph is 2.6 mm. (b) Curved fibres changing thickness across sharp bands These usually correspond to CL contrast (cf. Fig. 1). The horizontal edge of the photograph is 2.6 mm. (c) & (d) Veins with fibres connecting markers (O, T) across the vein. The horizontal edge of each photograph is 6.5 mm. (e) Vein in which fibres connect one set of markers (O) but fail to connect another set (T). The horizontal edge of the photograph is 6 5 mm (f) Vein in which fibres do not connect markers (O) The horizontal edge of the photograph is 6.5 mm.

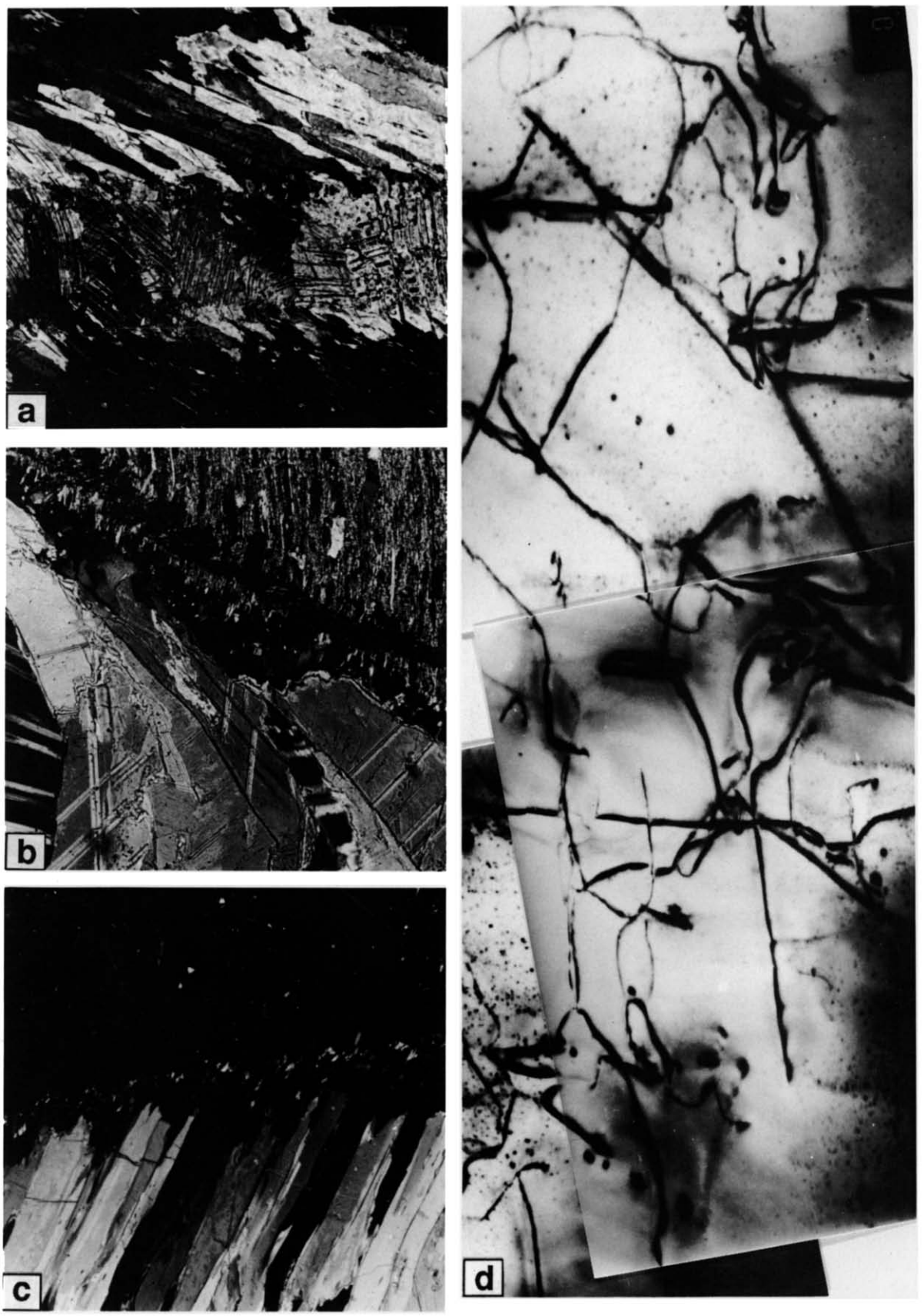


Fig. 4 (a) Vein with deformed, blocky core and fibrous rim The horizontal edge of the photograph is 1 mm. (b) & (c) Calcite–quartz selvage boundaries. See text for explanation. The horizontal edge of the photographs is 0.3 mm (d) TEM micrograph of typical intrafibre dislocation substructure, showing isolated curved dislocations, loops and nodal points. Scale bar is 1 $\mu$m

not connect markers across the vein (Figs. 1a & b, 2a & b and 3f). In both types, however, the sense of curvature of the fibres is always consistent with the apparent displacement of the markers. Both types are found in a single thin section, and even within a single vein (Figs. 2 and 3e). (It should be noted here that in the photographs shown in Figs. 1, 3 and 4 markers cannot always be correlated uniquely across the vein. This correlation was made using whole thin section micrographs for all markers referred to in the figure captions.)

TEM observations were made on typical fibres extending from the median line to the vein wall, curved approximately 40° with minor undulose extinction (Fig. 4d). The defect structure consists of minor *e*-twins, a few fluid inclusions and the following dislocation substructure: curved free dislocations, dislocation loops and isolated nodal points. Preliminary contrast analyses reveal $\langle 1\bar{1}02\rangle$ Burgers vectors, indicating most likely *f*- and *r*-slip ($\{10\bar{1}1\}\langle 1\bar{1}02\rangle$ and $\{0221\}\langle 1\bar{1}02\rangle$, respectively). Most of the dislocations can be shown to have climbed out of their glide planes, indicating dislocation creep processes. However, organized dislocation networks occur only to a limited extent. Dislocation density is around $10^8$ cm$^{-2}$, and fairly homogeneous over the fibre length. Fluid inclusions occur either along *e*-twins and isolated dislocations or as isolated bubbles, sometimes arranged in lines.

*'Blocky' veins.* About 20% of the veins studied contain large, more or less equant calcite crystals, giving them a blocky appearance. Veins changing laterally from fibrous to blocky, and veins with a blocky core overgrown by a fibrous outer part (Fig. 4a) are found locally. In a number of blocky veins grain *boundaries* have identical curvatures to fibre boundaries in the same sample (Figs. 1g & h). In addition, CL patterns of both fibrous and blocky veins are very similar, showing the same banding symmetrical about a median line with comparable sequences of intensity changes.

*Growth surface morphology.* All veins show a thin quartz–chlorite selvage between the calcite and the slate wall rock (see Figs. 4b & c), similar to the ones described in Ramsay & Huber (1983) and Williams & Urai (1989). Wherever small wall rock fragments are enclosed in complex veins initially consisting of more than one branch (as shown by CL zonation), the fragments have an identical quartz–chlorite selvage. In sharp vein tips the selvage from both sides of the vein coalesces into a thin, syntaxial quartz–chlorite vein approximately along the extension of the median line, containing occasional isolated calcite grains (Fig. 1e). Identical quartz–chlorite veins also occur unconnected to calcite veins in a number of cases (e.g. Fig. 2a).

At higher magnification, the quartz–chlorite selvage is often fibrous, with the fibres at a high angle to the vein wall, increasing in width toward the vein center. The boundary of the selvage with the calcite vein fill is irregular in shape, down to the submicron scale. The boundary generally has a dominant wavelength component of the same order of magnitude as the fibre diameter, and is generally non-interlocking with the vein material. When examined in detail, the fibre boundaries show a tendency to be located near points in this boundary which are closest to the median line.

## INTERPRETATION OF THE MICROSTRUCTURES

Following normal practice (e.g. Richter & Zinkernagel 1981, Dietrich & Grant 1985, Machel 1985, Solomon 1989) we interpret the bands of CL discontinuities as marking traces of a growth surface at successive growth increments, the differences in CL intensity being due either to changes in the geochemistry and temperature of the fluid (cf. Rye & Bradbury 1980), or to variation in crystal growth rate (ten Have & Heynen 1985). Both the symmetrical CL banding and the fibres extending across the median line are good evidence for antitaxial accretion of the veins, with simultaneous growth of all fibres from the median line towards the vein wall, and fracturing and growth at the quartz selvage–vein contact. The symmetry in the CL band shows that mean rates of accretion at opposing boundaries were more or less equal, and that the vein aspect ratio generally decreased during vein accretion. (Note that no information is present on the time-continuity of opening, and the veins may well have opened during several distinct periods of fluid movement, separated by periods of deformation without vein accretion.)

The available evidence suggests that a large part of the quartz–chlorite selvage grew syntaxially from the slate surface at an early stage of vein development, with possible additional growth at a later stage. On the other hand, the absence of calcite in the country rock around most veins suggests that calcite growth started with a nucleation stage. The difference between blocky and fibrous calcite morphologies may then be either due to differences in nucleation rates (producing differences in initial calcite grain size), or to the presence or absence of isolated fracture arrays during the initial opening stage (cf. Fig. 1e), the size of which determined the initial calcite grain size and shape.

As argued by Passchier & Urai (1988), vein accretion took place in a rock which was undergoing strongly non-coaxial deformation. The growing veins were rotating with respect to the instantaneous stretching axes, and depending on local variations in wall rock strengths, some veins could have deformed internally at different stages of growth. This agrees with some veins having a deformed center, overgrown by an undeformed rim, and is also supported by the TEM observations. These indicate plastic deformation of the fibres with low overall strains (less than a few per cent).

Optically continuous fibres with a curved shape can be formed by one or a combination of the following processes (see Williams & Urai 1989): (i) growth in a curved shape; (ii) plastic deformation of initially straight or less curved fibres; or (iii) process (ii), followed by grain boundary migration recrystallization. Williams & Urai

(1989) showed that lattice curvature in the case of initially straight fibres which are bent during subsequent deformation should be quite variable from grain to grain but generally less than the grain shape curvature However, in at least a number of veins in the present set of samples grain shape curvatures of up to 90° are accompanied by lattice curvature less than a few degrees in *all* grains (Fig. 3a). Thus we reject mechanism (ii) for these particular veins, but note that most veins have suffered a small amount of plastic deformation as shown by the common weak undulose extinction and the TEM dislocation substructure.

Deformation-induced recrystallization can also produce optically strain-free grains from bent originals by selective new grain growth through interiors of individual deformed grains (Williams & Urai 1989). However, the presence of a clear CL banding which is continuous over many grains is evidence against this interpretation in the samples studied. CL contrast in calcite is a sensitive function of Mn and Fe trace concentrations (ten Have & Heynen 1985). This type of zonation can reasonably be expected to be disturbed or destroyed by grain boundary migration, because of the ability of grain boundaries to transport segregated impurities through the material (e.g. Guillopé & Poirier 1979, Drury & Urai 1990). In recrystallized first generation veins in the samples studied and in other calcite tectonites CL zonation can indeed be shown to be modified by recrystallization. This argues against mechanism (iii) and we prefer the interpretation of fibre curvature in these veins as an original growth feature

As pointed out above, a criterion for testing the tracking hypothesis is to check if fibres connect material markers on both sides of the vein. In many of the veins studied this is indeed the case. Occasionally the smaller scale irregularities in CL banding provide internal markers which are also connected by the fibres. In other veins however, fibres do not connect material markers on both sides of the vein; therefore in these veins fibre curvature cannot be a simple consequence of the fibres tracking the full opening trajectory, by whatever mechanism. Similar conclusions were arrived at by Cox (1987) and Williams & Urai (1986, 1989).

An alternative explanation for the formation of 'non-tracking' fibres is by assuming a shear fracture at the site of the future vein, so that markers are displaced before the fibres start growing parallel to the opening trajectory. In the veins studied the mismatch between fibres and the markers is about one-tenth of the vein length, which is a common length–displacement ratio of faults. However, in this case one would expect the mismatch to be maximal at the middle of the vein, decreasing towards the ends, which is not the case in the samples studied. Also the case of the vein where only part of the fibres are non-tracking cannot be explained by this mechanism.

In summary, the fibres studied have a curvature formed during growth, but their long axes cannot have grown parallel to the opening direction in all cases. Thus, before vein fibres can be confidently used to analyse progressive deformation histories, we have to develop a better understanding of the processes involved in curved fibre growth

## A MODEL FOR THE GROWTH OF CURVED VEIN FIBRES

In what follows we present a simple model for crystal growth in a crack–seal environment. We consider the case of an antitaxial vein filled by a crack–seal mechanism The crack is localized along the vein–wall rock boundary, and growth takes place on the vein surface only. We make the following assumptions (these will be examined at a later stage): (1) the fracture is *completely filled* before the next cracking event occurs, and the vein is accreted by a large number of these events, all of more or less similar magnitude. (The magnitude of the opening vector need not be the same as the thickness of the growth increment, i.e. the crack may close partly during growth.) In addition we assume (2) that *crystal growth rates are isotropic*, that is, the growth surface propagates equally fast in all directions; and (3) that all interfaces considered have parallel lines of intersection, that is the model is *two-dimensional*.

Based on these assumptions, vein accretion will occur following the simple rules shown in Fig. 5. Here the vein–wall rock boundary is defined by the two planar segments A–B–C. The figure shows the details of three crack–seal events, along an opening trajectory described by non-parallel vectors. As a consequence of assumption (2), the growth surface remains parallel to its original shape, and the crack is not sealed simultaneously along its length. Considering the propagation of three representative grain boundaries (B1, B2 and B3) it is easily seen that two types of trajectories are possible: along lines perpendicular to the growth surface (B1 and B3) or along the bisector of two growth surfaces meeting in a corner (B2) These two modes of grain boundary propagation are a simple consequence of assumption (2) and they define all elements of the shape growth process described below.

Using the simple rules derived above we can now simulate vein growth using different combinations of starting grain diameter, crack geometry and opening trajectory. The simplest case of a planar crack is shown in Fig. 6(a). Here, successive crack–seal events produce fibrous crystals, which propagate *perpendicular to the growth surface*, independently of the opening history of the vein.

Let us now develop the simulations further and consider the crystal shapes produced using a crack shape defined by straight line segments (A–A′, Fig. 6b), along an opening trajectory composed of two straight parts. Assuming a starting grain boundary configuration as shown, it can be seen that most grain boundaries, (and thus the grain shapes) follow the opening trajectory quite closely. Thus using a simple set of assumptions to model vein accretion we can simulate the growth of curved fibrous crystal shapes which follow the opening trajectory of the vein.

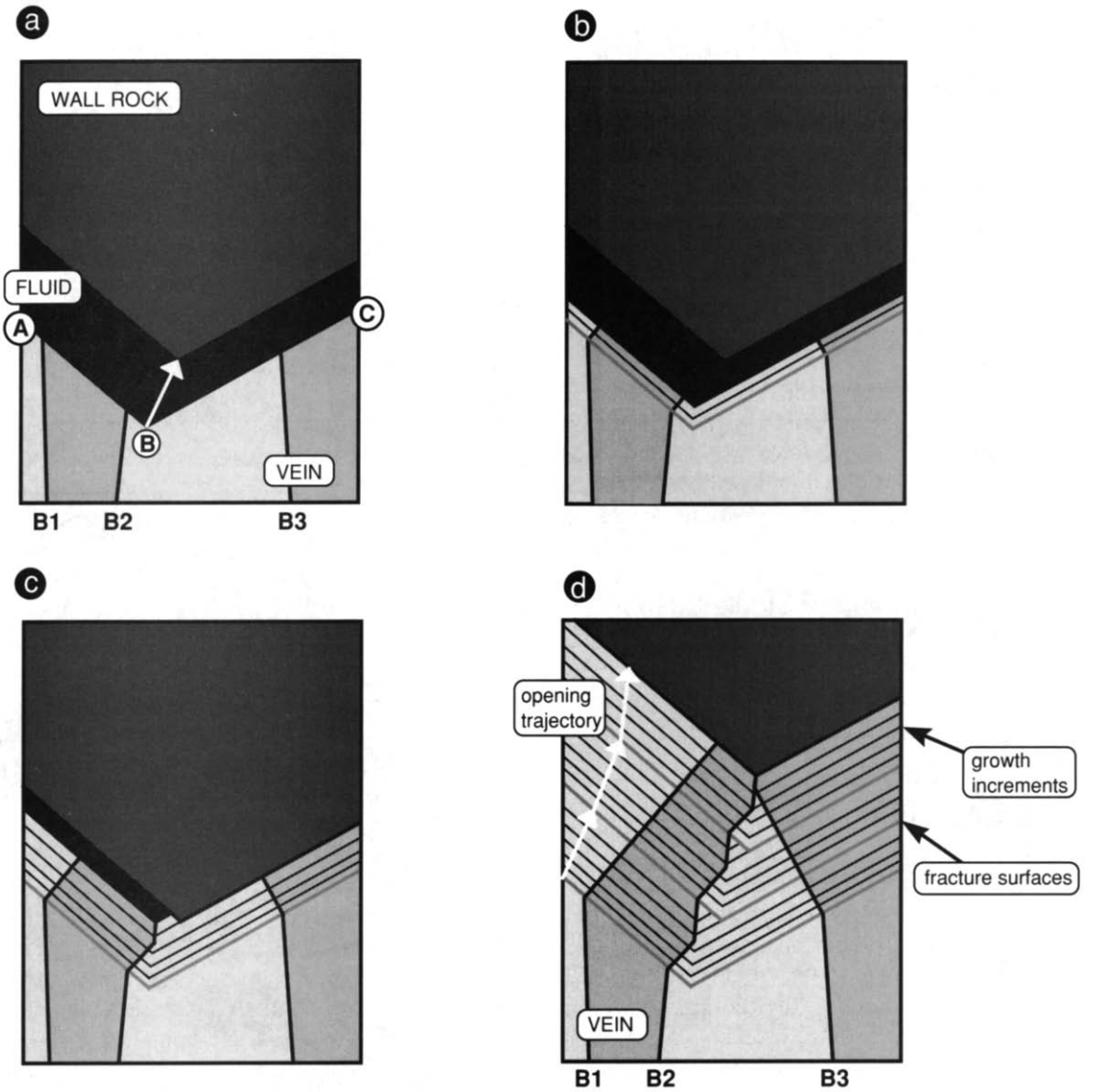


Fig 5 An illustration of grain boundary propagation in an antitaxial crack–seal vein, assuming isotropic growth kinetics. (a) Immediately after a cracking event (opening vector marked by white arrow). The wall rock–fluid interface is defined by the two planar sections A–B–C. Three representative grain boundaries in the vein material are marked B1, B2 and B3. (b) During the first sealing event, the growth surface has propagated equal distances everywhere. Therefore the three grain boundaries extend perpendicular to the growth surface. The grey line indicates the initial crack surface, and the thin black line marks the position of the growth surface at an earlier stage. (c) Sealing is almost complete. B1 and B3 have propagated perpendicular to the growth surface, but B2 has reached the corner in the growth surface and must from then on propagate along the bisectrix of the segments until the end of this seal event. (d) After three completed crack–seal events Note how B2 has started propagating perpendicular to the growth surface at the beginning of each sealing event, and continued along the bisectrix of the segments after reaching the corner in the growth surface

The procedure for the simulations is as follows. First one defines a median line, the wall rock boundary defined by a series of connected line segments, and an opening trajectory defined by a series of vectors. Then a number of grain boundaries are defined, connecting the median line and the wall rock boundary. The wall rock boundary is translated by the first opening trajectory vector, and the grain boundaries extended to 'fill the gap' following the rules outlined above. This process is repeated for all vectors of the opening trajectory. Note that we do not attempt to model the nucleation stage of the vein fill; the starting grain boundary configurations in the simulations are chosen arbitrarily. An infinite number of starting grain boundary configurations are possible with a given wall rock shape.

The simulations are characterized by the following geometrical elements (Fig. 6): opening increment length $x$, the wavelength $\lambda$ and amplitude $y$ of crack irregularities, and the angle $\alpha$ between the incremental opening vector and the local orientation of the crack surface. In addition we define $\beta$ as 2 arctan($\lambda/2y$). Variations in these parameters determine fibre morphology. For example, in Fig. 6(c) $y$ is decreased by a factor 3, in a situation otherwise identical to Fig. 6(b). It can be seen that although the fibrous shape is still maintained and the fibre long axis is slightly oblique to the enveloping

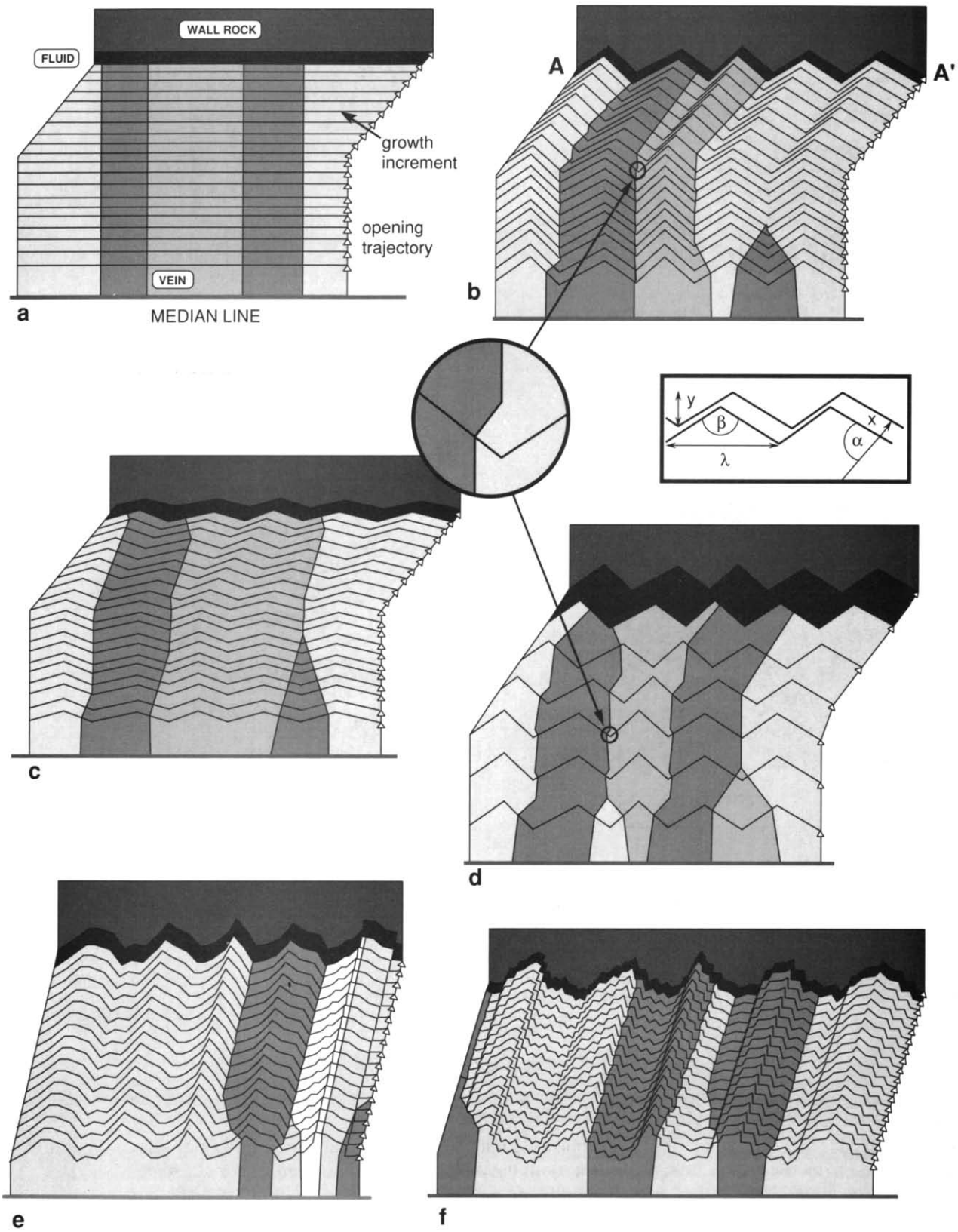


Fig. 6. Results of simulations of the development of antitaxial veins, using the model described in the text. (a) Vein growth in a planar crack. Note that fibres are straight irrespective of the shape of the opening trajectory. (b) The same situation as in (a), but with an irregular crack surface (A–A'), showing the growth of curved fibres which track the opening trajectory. The insert shows the geometrical elements discussed in the text. (c) As in (b) but with a lower value of $y$ (amplitude of crack irregularities). Note that fibres do not track the opening trajectory. (d) As in (b) but with a larger value of $x/\lambda$. Note that fibres do not track the opening trajectory. (e) Effect of more complicated crack shapes. Note that fibres track the opening trajectory, and that fibre boundaries tend to follow depressions in the growth surface. (f) Effect of a second wavelength component (of the order of $x$) in the crack surface. Note that the tendency for fibre boundaries to be located near the main depressions in the growth surface becomes less.

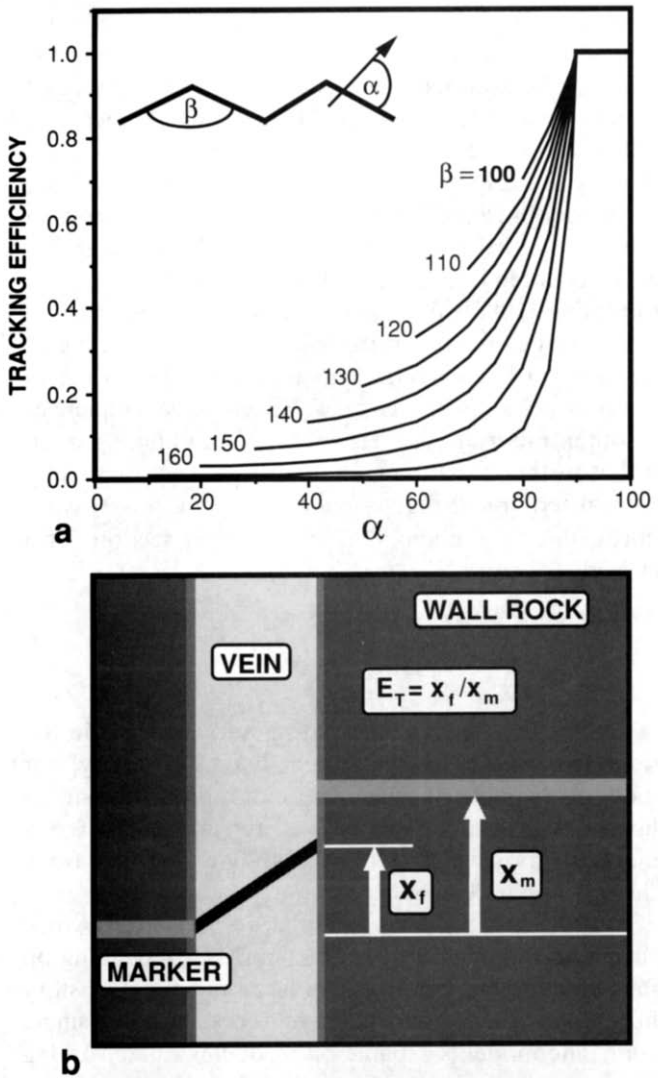


Fig. 7. (a) Tracking efficiency as a function of $\alpha$ and $\beta$. The insert shows the definitions of $\alpha$ and $\beta$ (b) Cartoon illustrating the definition of tracking efficiency $E_t$. See text for explanation

surface of the crack, the fibre does not track the opening trajectory. It is easily verified that in this case the main geometrical factor determining 'tracking efficiency' is the angle $\alpha$ between the incremental opening vector and the local orientation of the crack surface.

Another important factor in the model is illustrated in Fig. 6(d). Here we use the same crack shape and opening trajectory as in Fig. 6(b), but with a larger increment length $x$. It can be seen again that the fibres do not track the opening trajectory. The important parameter here is the ratio of the wavelength of the crack irregularities to the increment length, $x/\lambda$.

In summary, the model predicts, somewhat loosely, a 'tracking criterion' given by: $\alpha > 90°$ and $x \ll \lambda$. If this criterion is not met, fibres will track the opening direction only partially. We define tracking efficiency $E_t$ of a fibre as $E_t = x_f/x_m$, where $x_f$ is the vein parallel displacement recorded by the fibre and $x_m$ is the vein-parallel component of the net opening vector. For a simple symmetric crack geometry $E_t$ can be expressed as a function of the angles $\alpha$ and $\beta$ for $x \ll \lambda$. Figure 7 is a plot of $E_t$ as a function of $\alpha$, for different values of $\beta$. It can be seen that even for reasonably rough surfaces, at $\alpha < 90°$ the tracking efficiency quickly decreases to values well below 1.

Figure 6(e) further illustrates the consequences of more complicated crack shapes on fibre morphology. A number of aspects can be noted. First, as already seen in Fig. 6(a), grain boundaries have the tendency to grow towards the local depressions in the growth surface, (i.e. points closest to the median line). This means that in the case of a sufficiently fine-grained initial vein, a certain amount of growth selection may take place without the presence of anisotropic growth kinetics, the dominant fibre size being determined by the wavelength $\lambda$. If the initial crystal size is larger than $\lambda$, no increase of fibre thickness is possible, but the grain boundaries will propagate following the same rules as described above. For sufficiently large starting grain diameters blocky grains with their boundaries along the opening trajectory may be formed (cf. Fig. 1g).

In the case of more complicated natural crack geometries the wavelength $\lambda$ cannot be simply defined. However, from Fig. 6 it is clear that irregularities with a wavelength smaller than $x$ will not have a noticeable effect on grain boundary propagation. Here for practical purposes $\lambda$ can be taken at about $100x$. This is further illustrated in the simulation of Fig. 6(f), where the fibre boundaries follow second-order irregularities in the crack surface.

A further necessary condition for the simulation to work is that the crack can be opened without the two

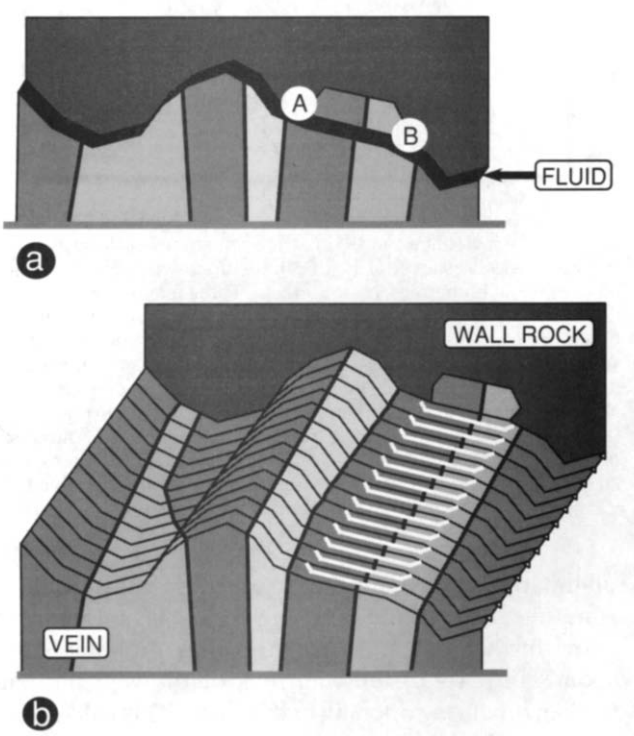


Fig. 8. Simulation similar to those in Fig 6, but with one section where vein and wall rock have interlocking shapes. (a) During the crack event the vein is fractured along A–B and in this section the crack is sealed by growth from both sides of the crack. Assuming the same rules as defined in Fig. 5 for both surfaces, and repeated fracturing along A–B, the resulting vein morphology is shown in (b). Broken lines indicate healed cracks in the fibre (in nature possibly marked by fluid inclusion trails) Note the small steps in the fibre boundary: these have already been described by Cox & Etheridge (1983)

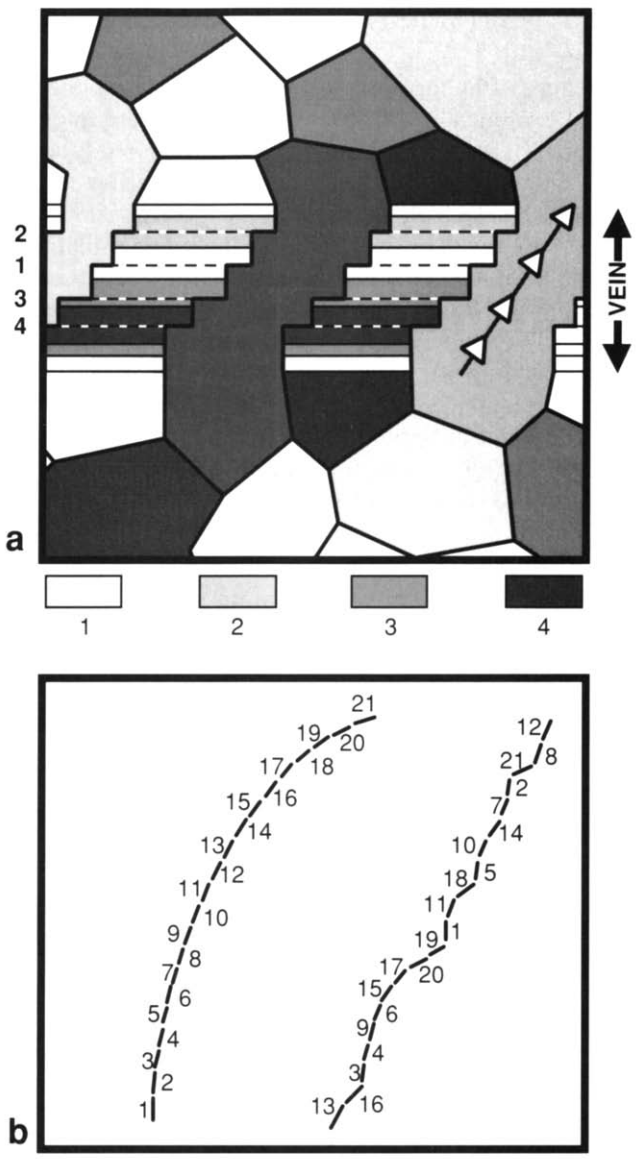


Fig 9 (a) Syntaxial crack–seal vein developed by delocalized cracking (after Cox & Etheridge 1983) The simulation was done assuming the same rules as shown in Fig 5, but with growth occurring simultaneously on both sides of the crack. Three grains are drawn to illustrate the expected optical continuity of a stretched crystal Two others are contoured according to age of accretion. Numbers refer to successive crack–seal events, dashed lines mark the sites of each seal and legend shows material added during the corresponding seal event. Note the complicated distribution of material added during the first seal event. (b) Curved opening trajectory composed of 21 successive numbered increments (left), and the fibre shape expected after syntaxial growth and delocalized cracking in a vein opening along this trajectory (right) See text for discussion

boundaries intersecting during opening. If this condition is not met, one of the two boundaries has to deform to allow further opening. In nature this probably corresponds to parts of the wall rock or the vein fill being broken off during opening of the crack. This will result in either small pieces of the wall rock being incorporated into the vein (cf. Fig. 1d) or internal fracturing of a fibre which may then continue growing by a syntaxial mechanism for some time (Fig. 8). It is indeed not uncommon to find vein-parallel trails of inclusions in antitaxial fibres indicating some degree of internal fracturing and syntaxial accretion

In an important paper, Cox & Etheridge (1983) described a number of processes by which syntaxial fibrous veins can be accreted They showed that fibres inclined to the vein wall may be formed by repeated de-localized fracturing in the vein Such fibres are referred to by Durney & Ramsay (1973) as 'stretched crystals'. Using the model presented in this paper it is also possible to simulate syntaxial vein growth This is illustrated in Fig 9(a). As noted by Durney & Ramsay (1973) and Cox & Etheridge (1983), fibre shape does not necessarily reflect the true opening trajectory because the fibre increments recording each incremental opening vector may not be stacked in the correct chronological sequence Another important property of this type of fibre growth is that in the case of *curved* opening trajectories, fully delocalized fracturing produces more or less *straight* fibres, due to random stacking of small sections of a curved trajectory (Fig. 9b).

## DISCUSSION

For the case of veins fracturing and accreting in the same structural setting, (syntaxially or antitaxially) our model is capable of producing natural-looking curved fibres. Although the model is quite simple, it offers a mechanism by which fibres may fully or partially track the opening trajectory.

In addition it provides a number of predictions which can be tested against natural examples. Depending on the details of the surface roughness and opening history fibres may or may not connect markers, even in a single vein. The model is capable of producing fibres varying from perpendicular to the wall rock to fully tracking. However it cannot produce fibres which show more offset than the markers or show an offset in the opposite direction to that of the markers. In all the examples

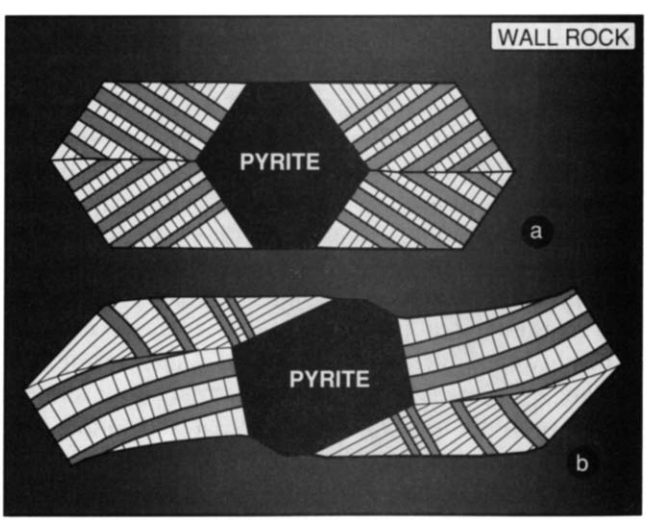


Fig 10 Simulation of antitaxial fibre growth in a pressure fringe around a rigid crystal Cracking and accretion take place at the crystal–fibre interface, which is assumed to be smooth In addition we assume no deformation of the pressure fringe. (a) There is no rotational component, and straight 'face-controlled' fibres are produced. (b) There is a rotational component during opening, producing curved fibres

examined by us to date, where suitable markers were present, this indeed seems to be the case. Fibres changing thickness during vein accretion (e.g. Fig. 3b) can be explained by the model by assuming changes in the crack shape during vein accretion, possibly by a stage of renewed growth of the quartz–chlorite selvage.

Veins opening with flat crack surfaces (cf. Fig. 6a) provide another situation against which the model can be tested. For example, fibrous quartz is frequently found in pressure fringes around euhedral pyrite crystals (Spry 1969, White & Wilson 1978, Ramsay & Huber 1983, p. 265). Here it is commonly inferred that accretion occurs at the quartz–pyrite interface, and fibres grow perpendicular to the pyrite faces, producing 'face controlled' fibres (fig. 14.10 in Ramsay & Huber, 1983). Using our model to simulate this situation (Fig. 10) it can be seen that depending on the presence of a rotational component in the motion of the wall rock with respect to the pyrite crystal, it predicts either straight or curved fibres growing perpendicular to the *growth surface* (see also Cox & Etheridge 1983). The model also predicts that the difference between 'face-controlled' and 'displacement-controlled' fibre morphologies (Ramsay & Huber 1983, p. 268) will be determined by the pyrite surface morphology.

At this stage we examine the assumptions of the model in more detail.

*Assumption* (1): cracks are filled completely before the next cracking event. In the absence of second-phase inclusion trails (see Ramsay 1980) we do not have any direct evidence for a crack–seal mechanism of accretion in the veins studied. Assumption (1) is certainly not always valid in nature, for example Fisher & Byrne (1990) described veins in which only part of the fibres grew fast enough to seal the crack in each event, and the space between these crystals was filled later by slower growing crystals. When assumption (1) is relaxed, the model can still generate fibrous morphologies with straight, non-parallel grain boundaries, but with fibres growing independently of the opening trajectory. Note however that a crack–seal process is thought to be essential in maintaining assumption (2), as explained below.

*Assumption* (2): crystal growth rates are isotropic. If a single crystal with smooth but arbitrarily cut (irrational), surfaces is placed in a slightly supersaturated solution, growth of this crystal can occur in two different ways (Bennema 1974, Sunagawa 1982, Bennema & van der Eerden 1987. (a) The initially smooth surface is gradually coarsened, and becomes covered by slow growing F faces (Hartman 1973). This anisotropic growth will result in F faces gradually determining crystal morphology: this is the commonly observed process by which euhedral crystals grow from solution. Growth mechanisms on these F faces are spiral growth at screw dislocation terminations or two-dimensional nucleation. (b) Above some critical value of temperature the flat faces undergo the so-called roughening transition (Bennema 1974). Under these conditions the formation of flat faces is not possible, and growth rates become a linear function of supersaturation (Nielsen & Toft 1984), the rate-limiting step being diffusion through the boundary layer at the crystal–fluid interface. Growth rates above the roughening transition tend to be isotropic, producing subspherical crystals.

In terms of crystal growth mechanisms, the fundamental difference between a crack–seal process and growth from a free fluid is that at the end of each crack–seal increment the crystals are forced to assume the (irrational) shape of the wall rock. As a consequence, growth in each seal event starts along these surfaces. These can in general be considered crystallographically rough, that is with a large density of atomic scale kinks on the surface.

Under the hydrothermal growth conditions considered, quartz and calcite growing in a free fluid tend to become euhedral. However, the fresh fracture surfaces after each cracking event can be considered rough until the first segments with F faces are formed on them. As shown by inclusion band separations, typical increment lengths in crack–seal veins are between 0.01 and 0.1 mm (Ramsay 1980, Cox 1987). Unfortunately no experimental or theoretical data are available on the rate at which rough faces become segmented, but it is reasonable to assume that for opening increments of up to a few tenths of microns the roughness of the growth surface will be maintained by the crack–seal mechanism. This will result in isotropic growth kinetics under conditions where this would not be predicted from conventional crystal growth considerations.

On the other hand, if the growth surface is not growing fast enough to seal the crack after each crack event, due to small differences in vein opening vs crystal growth rates, this may result in the switch between fibrous and euhedral, blocky veins (cf. Mawer 1987).

*Assumption* (3): the model is two-dimensional. Three-dimensional simulations using assumptions (1) and (2) are beyond the scope of the present study. However in the case of a symmetrical egg-box shaped wall rock–vein contact it can be quite easily verified that the same principles as derived in Fig. 10 will hold in general. In addition, the three-dimensional morphology of the growth surface has one essential property which is missing in our two-dimensional model. For crystal growth from a solution one has to assume fluid transport along the growth surface in order to deposit enough vein material to seal the crack. In Fig. 5 it can be seen that when the growth surface reaches the vein wall, no more transport along the growth surface is possible. In the three-dimensional situation however, fluid transport is expected to occur at a much later stage with transport along a complex tortuous path.

## CONCLUSIONS

Evidence for fibres having tracked the opening trajectory is provided by:

—optically undeformed primary fibres connecting markers across the vein;

—intermediate positions of the wall rock marked by CL or inclusion bands;

—microstructural evidence for localized cracking and accretion

The absence of any of these lines of evidence may lead to large errors of interpretation. We suggest that fibrous veins should be studied carefully before attempts are made to deduce progressive deformation histories from fibre shapes.

A simple model, assuming crack–seal accretion and isotropic growth kinetics is capable of explaining the range of presently documented fibrous vein microstructures.

*Acknowledgements*—We thank P. Hartman, S. F. Cox, W. D. Means, M. Ellis, C. Woensdregt and E. van der Voort for illuminating discussions on crystal growth and on vein fibres, and for thoughtful reviews which much improved the manuscript. Financial support to J. L. Urai from a C & C Huygens fellowship of The Netherlands Organization for the Advancement of Pure Research (NWO) is gratefully acknowledged. P. F. Williams was supported by a National Sciences and Engineering Research Council (NSERC) Operating Grant. Electron microscopy was carried out at the EM facilities at Utrecht supported by NWO.

## REFERENCES

Beach, A. 1977. Vein arrays, hydraulic fractures and pressure solution structures in a deformed flysch sequence, S. W. England. *Tectonophysics* **40**, 201–225.

Bennema, P. 1974. Crystal growth from solution—theory and experiment. *J. Crystal Growth* **24/25**, 76–83.

Bennema, P. & Eerden, J. P. van der 1987. Crystal graphs, Connected nets, roughening transition and the morphology of crystals. In: *Morphology of Crystals, Part A* (edited by Sunagawa, I.). Terrapublications, Tokyo, 1–75.

Beutner, E. C. & Diegel, F. A. 1985. Determination of fold kinematics from syntectonic fibres in pressure shadows, Martinsburg slate, New Jersey. *Am. J. Sci.* **285**, 16–50.

Bosworth, W. & Kidd, W. S. F. 1985. Thrusts, melanges, folded thrusts and duplexes in the Taconic foreland. In: *New York State Geological Association 57th Annual Meeting Field Trip Guidebook* (edited by Lindemann, R.). Skidmore College, Saratoga, New York.

Bosworth, W. & Vollmer, F. W. 1981. Structures of the medial Ordovician flysch of Eastern New York: Deformation of synorogenic deposits in an overthrust environment. *J. Geol.* **89**, 551–568.

Cox, S. F. 1987. Antitaxial crack-seal vein microstructures and their relationship to displacement paths. *J. Struct. Geol.* **9**, 779–787.

Cox, S. F. & Etheridge, M. A. 1983. Crack-seal fibre growth mechanisms and their significance in the development of oriented layer silicate microstructures. *Tectonophysics* **92**, 147–170.

Cox, S. F. Etheridge, M. A. & Wall, V. J. 1986. The role of fluids in syntectonic mass transport and the localization of metamorphic vein-type ore deposits. *Ore Geol. Rev.* **2**, 65–86.

Dietrich, D. & Grant, P. R. 1985. Cathodeluminescence petrography of syntectonic quartz fibres. *J. Struct. Geol.* **7**, 541–553.

Drury, M. & Urai, J. L. 1990. Deformation related recrystallization processes. *Tectonophysics* **172**, 235–253.

Durney, D. W. & Ramsay, J. G. 1973. Incremental strains measured by syntectonic crystal growths. In: *Gravity and Tectonics* (edited by De Jong, K. A. & Scholten, R.). John Wiley, New York, 67–96.

Ellis, M. 1986. The determination of progressive deformation histories from antitaxial syntectonic crystal fibres. *J. Struct. Geol.* **8**, 701–709.

Fisher, D. & Bryne, T. 1990. The character and distribution of mineralized fractures in the Kodiak formation, Alaska: Implications for fluid flow in an underthrust sequence. *J. geophys. Res.* **95 (B6)**, 9069–9080.

Grigor'ev, D. P. 1965. *Ontogeny of Minerals*. S. Monson, Jerusalem.

Guillopé, M. & Poirier, J. P. 1979. Dynamic recrystallization during creep of single crystalline halite: an experimental study. *J. geophys. Res.* **84(B10)**, 5557–5567.

Hartman, P. 1987. Modern PBC theory. In: *Morphology of Crystals, Part A* (edited by Sunagawa, I.). Terrapublications, Tokyo, 269–319.

Have, T. ten & Heynen, W. M. M. 1985. Cathodeluminescence activation and zonation in carbonate rocks: an experimental approach. *Geologie Mijnb.* **64**, 297–310.

Machel, H. G. 1985. Cathodeluminescence in calcite and dolomite and its interpretation. *Geosci. Can.* **10**, 139–147.

Mawer, C. K. 1987. Mechanics of formation of gold-bearing quartz veins, Nova Scotia, Canada. *Tectonophysics* **136**, 99–119.

Nielsen, A. E. & Toft, J. M. 1984. Electrolyte crystal growth kinetics. *J. Crystal Growth* **67**, 278–288.

O'Hanley, D. S. 1987. Deformation-free growth of NaCl cross-fiber veins: implications for syntectonic growth. *Geol. Soc. Am. Abs. w. Prog.* **19**, 237.

Passchier, C. W. & Urai, J. L. 1988. Vorticity and strain analysis using Mohr diagrams. *J. Struct. Geol.* **10**, 755–763.

Pluijm, B. A. van der 1984. An unusual 'crack-seal' vein geometry. *J. Struct. Geol.* **6**, 593–597.

Ramsay, J. G. 1980. The crack-seal mechanism of rock deformation. *Nature* **284**, 135–139.

Ramsay, J. F. & Huber, M. I. 1983. *The Techniques of Modern Structural Geology, Volume 1: Strain Analysis*. Academic Press, London.

Richter, D. K. & Zinkernagel, U. 1981. Zur Anwendung der Kathodoluminescenz in der Karbonatpetrographie. *Geol. Rdsch.* **70**, 1276–1302.

Rye, D. M. & Bradbury, H. J. 1988. Fluid flow in the crust: an example from a Pyrenean thrust ramp. *Am. J. Sci.* **288**, 197–235.

Solomon, S. F. 1989. The early diagenetic origin of lower Carboniferous mottled limestones (pseudobreccias). *Sedimentology* **36**, 399–418.

Spry, A. 1969. *Metamorphic Textures*. Pergamon Press, Oxford.

Sunagawa, I. 1982. Morphology of crystals in relation to growth conditions. *Estudios Geol.* **38**, 127–134.

White, S. H. & Wilson, C. J. L. 1978. Microstructure of some quartz pressure fringes. *Neues Jb. Miner. Abh.* **134**, 33–51.

Williams, P. F. & Urai, J. L. 1986. Curved vein fibres: an alternative explanation (Abs.). *International Conference on Tectonic and Structural Processes*, Utrecht.

Williams, P. F. & Urai, J. L. 1989. Curved vein fibres: an alternative explanation. *Tectonophysics* **158**, 311–333.